iScience

CellPress
OPEN ACCESS

Article

Plasma cells arise from differentiation of clonal lymphocytes and secrete IgM in Waldenström macroglobulinemia

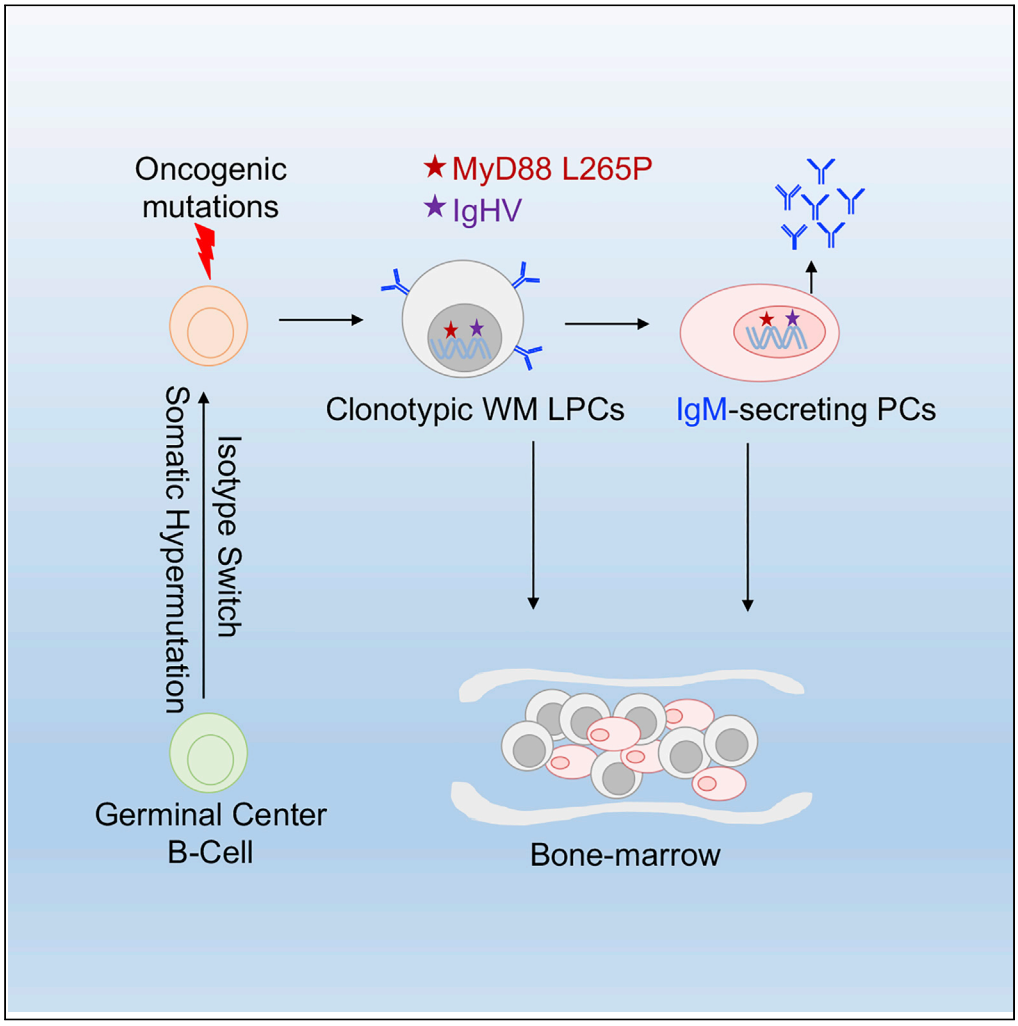

Jun Hee Lim, James Q. Wang, Fiona Webb, ..., Abhimanu Pandey, Si Ming Man, Dipti Talaulikar

dipti.talaulikar@act.gov.au

Highlights

Clonal differentiation of malignant LPCs gives rise to PCs in WM

LPCs and PCs harbor MYD88 L265P mutation and express the same IgHV sequence

PCs are the major source of IgM in WM

Lim et al., iScience 25, 104856
August 19, 2022
https://doi.org/10.1016/j.isci.2022.104856

iScience

CellPress
OPEN ACCESS

Article

Plasma cells arise from differentiation of clonal lymphocytes and secrete IgM in Waldenström macroglobulinemia

Jun Hee Lim,[1,2,3] James Q. Wang,[4] Fiona Webb,[5] Kartik Saxena,[1] Daniel Enosi Tuipulotu,[3] Abhimanu Pandey,[3] Si Ming Man,[3] and Dipti Talaulikar[1,2,3,6,*]

SUMMARY

Waldenström macroglobulinemia (WM) is characterized by bone marrow infiltration with malignant lymphoplasmacytic cells (LPCs), a smaller population of plasma cells (PCs), and hypersecretion of IgM monoclonal protein. Here, we show that CD45^{low}, CD38^{+}, and CD138^{+} PCs and CD45^{high}, CD38^{-}, CD138^{-}, CD19^{+}, and CD20^{+} LPCs carry a heterozygous L265P mutation in the Toll-like receptor signaling adaptor MYD88. Both PCs and LPCs express the same auto-reactive IgHV sequences, suggesting a similar clonal origin and role for auto-antigens in WM cell survival. PCs are primarily responsible for IgM production even without substantial cell proliferation. When cultured in isolation, LPCs give rise to more differentiated PCs and secrete less IgM. Our analyses suggest that malignant PCs arise from the clonal LPC population, and are primarily responsible for IgM secretion in WM. Targeting malignant PCs may have therapeutic benefits in the treatment of WM and improve the duration of response and potentially, survival.

INTRODUCTION

Waldenström macroglobulinemia (WM) is a rare subtype of mature indolent B cell lymphoma, a cancer of mature B lymphocytes which is characterized by the presence of monoclonal immunoglobulin M (IgM) hypersecretion and the accumulation of heterogeneous malignant B cells in the bone marrow (BM) (Owen et al., 2003; Lynch et al., 2017; El-Ayoubi et al., 2017). It is classified as a malignancy with plasmacytic differentiation. Two distinct subsets of cells in WM can be identified depending on their morphology and immunophenotypic characteristics: a predominant population of lymphoplasmacytic cells (LPCs) which are phenotypically defined as CD19^{+}, CD20^{+}, and CD138^{-} and plasma cells (PCs) which are phenotypically defined as CD38^{+} and CD138^{+}, with lower levels of CD45 and CD19 and variable CD20 (Lin et al., 2005; Morice et al., 2009; Wada et al., 2016). In WM, the abnormal LPCs cause cytopenias due to gradual marrow infiltration. PCs are non-dividing terminally differentiated mature effector B cells that produce antibodies and contribute to immunity (Calame, 2001). PCs are unlikely to contribute significantly to cytopenias, due to their low proportions in the bone marrow (El-Ayoubi et al., 2017).

Mutations in the gene encoding the Toll-like receptor adaptor protein called myeloid differentiation primary response gene 88 (MYD88) occur in over 90% of patients with WM (Xu et al., 2013; Varettoni et al., 2013), making WM one of the rare lymphomas with a signature single mutation that can be used to diagnose cases in clinical practice. The most common *Myd88* mutation results in a leucine-to-proline substitution at position 265, named MYD88 L265P (Ngo et al., 2011). This mutation is not found in normal tissues of patients with WM or in B cells from healthy donors, suggesting that a potential oncogenic event in MYD88 is linked to malignant transformation of B cells in patients with WM (Xu et al., 2014). MYD88 contains three main domains, an N-terminal death domain (DD), an intermediate linker domain (ID), and a C-terminal Toll/interleukin-1 receptor-like domain (TIR). Following ligand binding, the cytoplasmic TIR domain of Toll-like receptors associates with TIR domain of MYD88 via a homotypic TIR-TIR interaction (Dunne et al., 2003). IL-1 receptor-associated kinases (IRAKs) are then recruited to MYD88 via a DD domain interaction and is autophosphorylated, leading to the activation of both the canonical NF-kB pathway and the mitogen-activated protein kinase pathway to promote cell survival (Muzio et al., 1997; Lin et al., 2010). The MYD88 L265P mutation is located within the MYD88 TIR domain and causes constitutive formation of the TLR-MYD88-IRAKs signaling complex to induce aberrant activation of

[1]Haematology Translational Research Unit, Canberra Hospital, Canberra, Australia

[2]ANU Medical School, College of Medicine and Health, Australian National University, Canberra, Australia

[3]Division of Immunology and Infectious Disease, The John Curtin School of Medical Research, The Australian National University, Canberra, Australia

[4]ACRF Department of Cancer Biology and Therapeutics, The John Curtin School of Medical Research, The Australian National University, Canberra, Australia

[5]Department of Diagnostic Genomics, ACT Pathology, Canberra, Australia

[6]Lead contact

*Correspondence: dipti.talaulikar@act.gov.au

https://doi.org/10.1016/j.isci.2022.104856

NF-κB signaling, promoting malignant cell proliferation in WM (Treon et al., 2012). In addition, MYD88 L265P mutation can trigger B cell receptor (BCR) pathway crosstalk via a MYD88-TLR9-BCR (IgM) supercomplex resulting in chronically activated BCR signaling, which in turn can promote cell survival via NF-κB and mTOR signaling (Phelan et al., 2018).

An increased level of IgM paraprotein or monoclonal IgM in circulation of patients with WM may cause symptomatic hyperviscosity (Lynch et al., 2017), which is observed in up to 30% of patients with WM and manifests as neurological and bleeding symptoms (Mehta and Singhal, 2003; Stone and Bogen, 2012). The serum IgM levels inducing hyperviscosity-related symptoms are diverse in individual patients with WM ("symptomatic threshold") (Fahey et al., 1965) but generally WM guidelines recommend initiation of plasmapheresis at levels of >60 g/L even in asymptomatic patients with WM (Gustine et al., 2017b).

Identifying the cellular fraction(s) responsible for the secretion of IgM is therefore important in understanding the pathogenesis of WM and could potentially provide new targets or avenues for treatment. Small retrospective studies have shown a lack of concordance between LPC numbers in the bone marrow and IgM levels (Pasricha et al., 2011; De Tute et al., 2013). There is evidence of concordance between PC numbers in the BM and IgM levels suggesting that PCs are the primary secretors of IgM (Pasricha et al., 2011). Despite this clear relationship, PCs in WM have not been comprehensively analyzed to determine their immunophenotypic and molecular features, and secretory function. Here, we characterized the immunophenotype, molecular genetics, and secretory function of PCs and LPCs from WM.

RESULTS

Quantification of plasma cell and lymphoplasmacytic cell populations in WM cell lines and patients with WM

To investigate the characteristics of PCs and LPCs in WM cells and patients, we sorted PCs and LPCs from WM cell lines and patients using a conservative sorting strategy (Figure 1A). We analyzed the two WM cell lines and identified 10.16% PCs ($CD45^{low}/CD38^{+}/CD138^{+}$) and 11.72% LPCs ($CD45^{high}/CD138^{-}/CD19^{+}/CD20^{+}$) in MWCL-1 and 1.48% PCs ($CD45^{low}/CD38^{+}/CD138^{+}$) and 29.03% LPCs ($CD45^{high}/CD138^{-}/CD19^{+}/CD20^{+}$) in BCWM.1. We did not include $CD38^{-}/CD138^{+}$ cells regardless of CD45 expression level to clearly distinguish features of PCs and LPCs (Figure 1B). We also analyzed three BM aspirates of patient with WM using CD319 antibody instead of CD138 to gate PCs, because anti-CD138 antibody (DAKO) does not bind to PCs in frozen patient samples and CD319 is reported to be an alternative PC marker in the presence of anti-CD138 immunotherapeutic drugs (Soh e al., 2021). We identified in three patients: 0.82% PCs and 7.52% LPCs in patient 1, 3.43% PCs and 2.64% LPCs in patient 2, 16.28% PCs and 4.98% LPCs in patient 3 (Figure 1C). These results show that the portions of PCs and LPCs are variable in WM cell lines and patient samples.

The MYD88 L265P mutation is found in WM cell lines and the same IgHV isotype is conserved between PCs and LPCs

Given that the MYD88 L265P mutation is not found in normal tissues of patients with WM or in B cells from healthy donors, we used PCR to identify the presence or absence of this mutation in PCs and LPCs (Figure 2A). We found that the MYD88 L265P mutation was present in both FACS-sorted PC and LPC fractions of both WM cell lines (Figures 2B and 2C). Next, we investigated the IgHV sequence to verify clonally rearranged immunoglobulin (Ig) using FR3 primers targeting the Ig heavy chain. The expression of the same IgHV sequences was found in PCs and LPCs (IgHV3-15*01 and IgHV3-23*01 in MWCL-1 and BCWM.1, respectively) (Figure 2D). These results suggest that the PCs in the two WM cell lines were part of the malignant clone, and likely derived from differentiation of clonal LPCs carrying the MYD88 L265P mutation.

Chromosomal copy number changes are detected in MWCL-1 cell line and two patients with WM using SNP microarray

Deletions in chromosome 2p21, 17p11-p13.2, and 17q25.1–17q25.3 have been reported in MWCL-1 and its parental cells (Hodge et al., 2011). To investigate whether these copy number abnormalities are present in WM cells and patients, we performed DNA SNP microarray on the PCs and LPCs from two WM cell lines and six patients. In MWCL-1, the copy number losses of 11q23.2, 17p11.2-p13.1, and 17q25.1-q25.3, and the copy number gain of 11q23.2-q25 were detected in 95% of the clones from both PCs and LPCs (Table 1 and Figure S1), and the copy number loss of 6q11.1-q27 and 8p12-p23.3 was detected only in less than 10% of both populations (Table 1). We did not detect the copy number change of chromosome 2 in the MWCL-1 cell line as previously reported (Hodge et al., 2011).

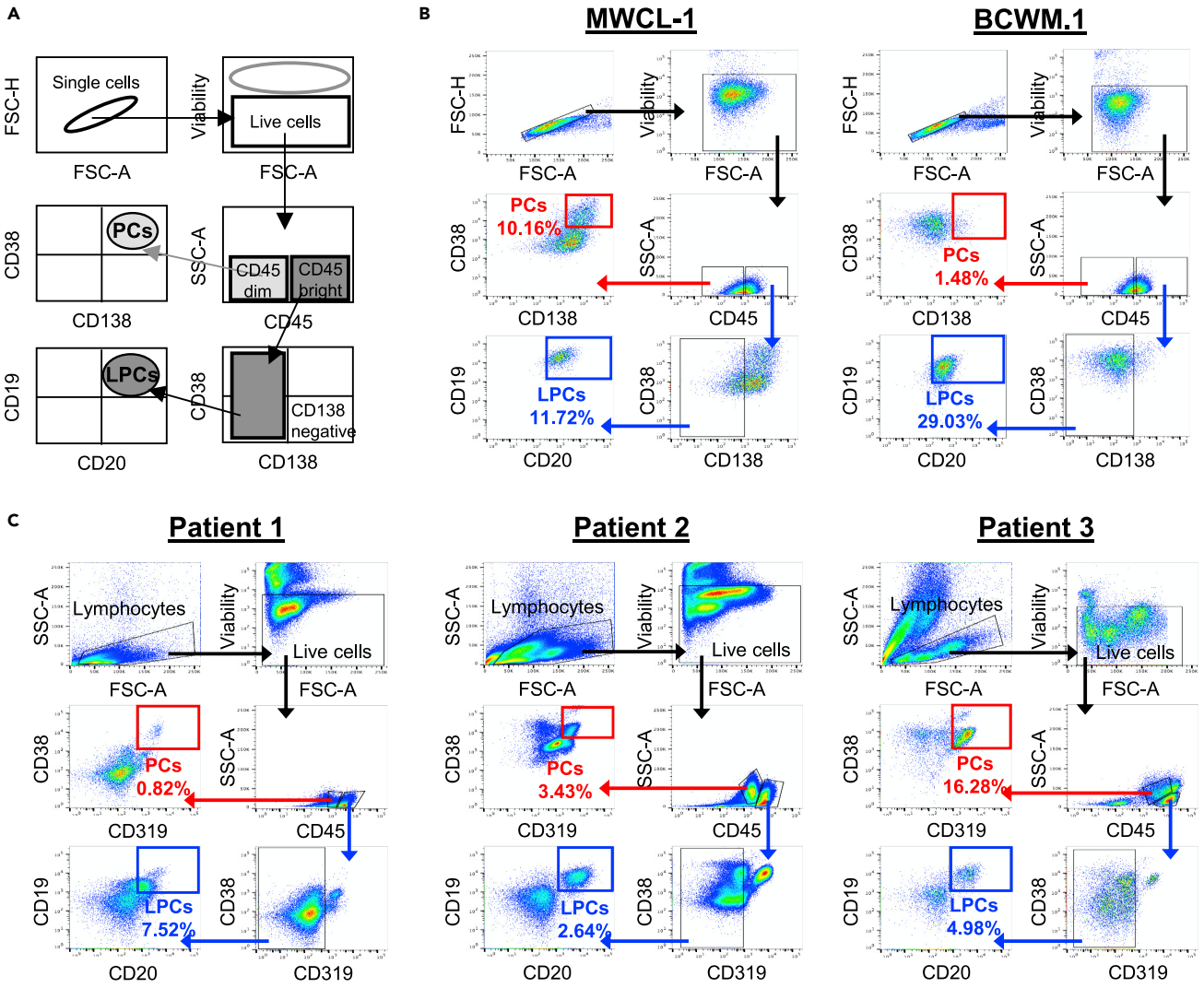

Figure 1. Gating strategy for sorting plasma cells (PCs) and lymphoplasmacytic cells (LPCs) from WM cell lines and patient bone marrow

(A) A graphical representation of the gating strategy.

(B) The application of this gating strategy for two WM cell lines. Single cells were gated using forward scatter (FSC-H vs. FSC-A) and dead cells showing positive signal for fixable viability stain 700 were excluded. From $CD45^{low}$ population gate, CD138 and CD38 co-expression was used to identify PCs. From $CD45^{high}$ population gate, the LPCs that showed negative staining for CD138 were first identified. The LPCs were further segregated based on CD19 and CD20 co-expression (LPC).

(C) Three WM patient samples were immunophenotyped using same gating strategy, except staining with CD319 Ab instead of CD138 Ab for PCs. The percentages of PCs and LPCs were calculated from live lymphocytes.

Of the six patients with WM, chromosomal changes were detected in two patients. In patient 1, AOH (absence of heterozygosity) of 3p21.31-p26.3 was found in 60% to 70% of PCs and in only 25% of LPCs and the copy number loss of 9p13.2 was found in LPCs alone (Table 1 and Figure S2). In patient 4, AOH in 6q13-q15 and 7q31.1–32.3 and the copy number loss of 22q11.22 were found at 100% of the clone from both cell populations suggesting germline changes, likely benign, in this patient (Table 1 and Figure S3). We did not detect any chromosomal copy number changes in the BCWM.1 cell line and the four remaining patients with WM including patient 2, patient 3, patient 5, and patient 6 (Table 1).

Copy number changes and AOH were identified in MWCL-1 and two patient samples, patient 1 and patient 4. Of these, MWCL-1 and patient 4 had no differences in SNP microarray between paired PCs and LPCs. Only patient 1 had a differential result in the PC and LPC fractions. Patient 1 showed loss of 9p13.2 in the LPCs but not in the PCs. The genes located in the affected short arm of chromosome 9 include

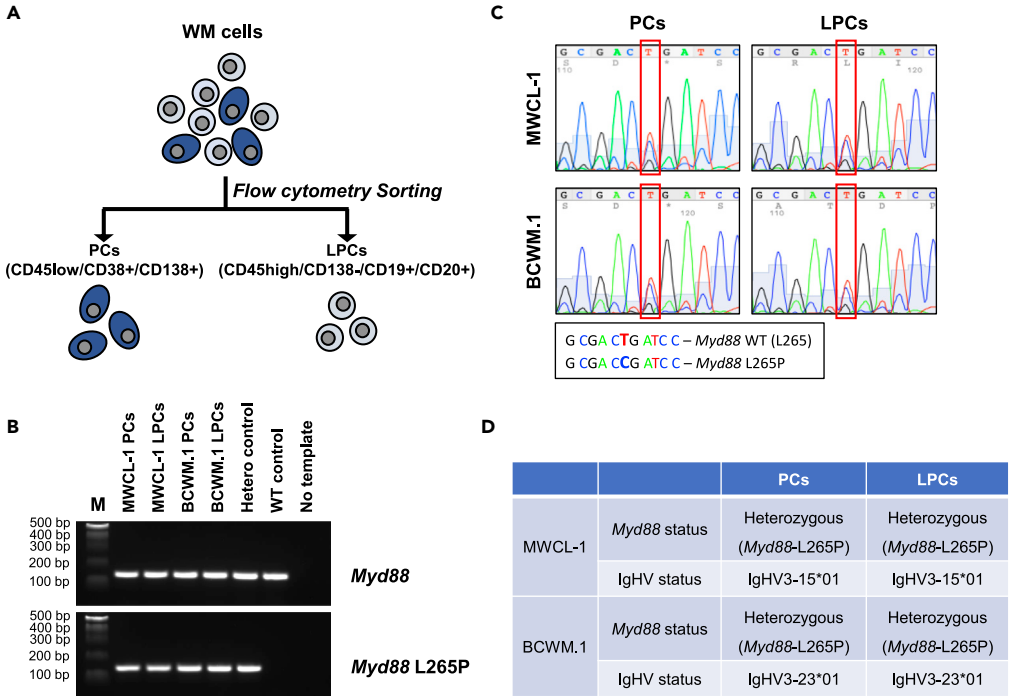

D

		PCs	LPCs
MWCL-1	*Myd88* status	Heterozygous (*Myd88*-L265P)	Heterozygous (*Myd88*-L265P)
	IgHV status	IgHV3-15*01	IgHV3-15*01
BCWM.1	*Myd88* status	Heterozygous (*Myd88*-L265P)	Heterozygous (*Myd88*-L265P)
	IgHV status	IgHV3-23*01	IgHV3-23*01

Figure 2. Determination of *Myd88* mutation status and IgHV isoform by PCR

(A) Schematic representation of isolation of PCs and LPCs from WM cell lines using FACS.

(B) *Myd88* PCR against genomic DNA extracted from PCs and LPCs (lane 1. MWCL-1 PCs; lane 2. MWCL-1 LPCs; lane 3. BCWM.1 PCs; lane 4, BCWM.1 LPCs; lane 5. heterozygous control; lane 6. wild-type control; lane 7. no template). The *Myd88* primer set targets both wild-type and L265P mutant, and *Myd88* L265P primer set targets L265P mutant only.

(C) Sanger sequencing result of *Myd88* PCR amplicons from BCWM.1 and MWCL-1 PCs and LPCs.

(D) Summary of *Myd88* and IgHV PCR amplicon sequencing.

RNF38, MELK, ALL3, FBXO10, and PAX5. Overall, our results indicate that LPCs and PCs are derived from the same parental population and carry similar SNP microarray changes. No firm conclusions can be drawn on the basis of the one patient sample that had variable results between the LPC and PC population.

Somatic mutations identified by next-generation sequencing

Next-generation sequencing was performed to determine the somatic mutations in PCs and LPCs of the two WM cell lines (MWCL-1 and BCWM.1) and two WM patient samples (patient 3 and patient 4) using customized capture library covering approximately 200 genes, which are known to be related to tumorigenesis and lymphomagenesis. The mutational profile in the cellular compartments of the cell lines and the patient samples was analyzed. Somatic T/C mutation in MYD88 resulting in an L265P substitution was detected in both populations of two WM cell lines and patient 4, but not in patient 3 (Table 2). The truncated CXCR4 mutation, S338X was detected in both PC and LPC populations in patient 4 (Table 2). The frameshift mutation on ARID1A, which is a member of the switch/sucrose nonfermentable (SWI/SNF) family to regulate chromatin remodeling and modulate gene regulation, was detected in both cell populations of patient 4 (Guan et al., 2011). The ARID1A mutation has been reported to be found in 17% of patients with WM (Hunter et al., 2014). Mutations in NOTCH2 were found in all other samples except LPCs in the MWCL-1 cell line. PRDM2 gene was mutated in both populations in the two WM cell lines and in patient 4, and the LPCs population of patient 3. In addition, mutations in ALK, ATM, IKZF3, LONP1, MKI67, MTHER, OBSCN, PLEKHG1, SYNE1, TET2, TNFRSF11A, UNC80, and ZFHX4 were recurrent findings in all eight cell populations (two cell fractions from two cell lines and two patients) that were tested.

Our results indicate that most somatic mutations were present in both PCs and LPCs from patients and cell lines except for PRDM2, KMT2B, and MAP2. The PRDM2 mutation was seen in LPCs of patient 3 but not in PCs. The KMT2B mutation was only detected in PCs of BCWM.1 cell line and the MAP2 mutation was found in PCs of MWCL-1 cell line.

Table 1. Chromosomal copy number changes in PCs and LPCs using SNP microarray

Sample	Cell fraction	Chromosome	Start	Stop	Size	Loss/ Gain	Frequency in sample
MWCL-1	CD138+	6q11.1-q27	62009419	170765619	108 MB	Loss	<10%
		8p23.3-p12	240792	33495305	33 MB	Loss	<10%
		11q23.2	113953295	114324183	0.37 MB	Loss	NA
		11q23.2-q25	114494276	134945120	20.4 MB	Gain	>95%
		17p13.1-p11.2	7290821	20717265	13.4 MB	Loss	>95%
		17q25.1-q25.3	73240165	76049375	2.8 MB	Loss	>95%
	CD19+	6q11.1-q27	62009419	170765619	108 MB	Loss	<10%
		8p23.3-p12	240792	33495305	33 MB	Loss	<10%
		11q23.2	113953295	114324183	0.37 MB	Loss	NA
		11q23.2-q25	114494276	134945120	20.4 MB	Gain	>95%
		17p13.1-p11.2	7290821	20717265	13.4 MB	Loss	>95%
		17q25.1-q25.3	73240165	76049375	2.8 MB	Loss	>95%
BCWM.1	CD138+	No copy number change detected					
	CD19+	No copy number change detected					
Patient 1	CD138+	3p26.3-p21.31	141149	49162550	49 MB	Loss	60%–70%
	CD19+	3p26.3-p21.31	141149	49162550	49 MB	Loss	25%
		9p13.2-p13.2	36325964	37749213	1.42 MB	Loss	50%
Patient 2	CD138+	No copy number change detected					
	CD19+	No copy number change detected					
Patient 3	CD138+	No copy number change detected					
	CD19+	No copy number change detected					
Patient 4	CD138+	6q13-q15	77707107	92340802	14.6 MB	Loss	100%
		7q31.1-q32.3	112702416	130614967	17.9 MB	Loss	100%
		22q11.22	22696066	23258488	0.56 MB	Loss	100%
	CD19+	6q13-q15	77707107	92340802	14.6 MB	Loss	100%
		7q31.1-q32.3	112702416	130614967	17.9 MB	Loss	100%
		22q11.22	22696066	23258488	0.56 MB	Loss	100%
Patient 5	CD138+	No copy number change detected					
	CD19+	No copy number change detected					
Patient 6	CD138+	No copy number change detected					
	CD19+	No copy number change detected					

Mutations in the gene encoding FCGR3A were detected in all samples. Among these mutations of FCGR3A, the FCGR3A-158V/F polymorphism is implicated in modulating IgG antibody binding and activation. It has been reported that the phenylalanine alone (F/F) is associated with decreased response to rituximab, due to the less binding affinity for IgG1 than valine homologous (V/V) or heterozygous (V/F) at 158 of FCGR3A (Koene et al., 1997; Weng and Levy, 2003). The FCGR3A F/F polymorphism was detected in PCs and LPCs from MWCL-1 cell line and patient 4, and the F/V polymorphism was detected in both

Table 2. Quantitation of somatic mutations identified in PCs and LPCs using NGS

	MWCL-1		BCWM.1		Patient 3		Patient 4	
	CD138+	CD19+/CD138-	CD138+	CD19+/CD138-	CD138+	CD19+/CD138-	CD138+	CD19+/CD138-
FCGR3A	2	2	1	1	3	3	2	2
NOTCH2	1		1	1	1	1	1	1
PRDM2	1	1	2	3		1	1	1
DNMT3A	1	1			1	1	1	1
MTHER	1	1			1	1	1	1
MYD88	1	1	1	1			1	1
OBSCN			3	3	1	1	2	2
TET2	2	2	2	2			2	2
ALK	2	2			1	1		
ATM			1	1			1	1
IKZF3			1	1			1	1
LONP1	2	2					1	1
MKI67	3	3					1	1
MTRR	3	2					4	3
PLEKHG1			1	1			3	3
SYNE1			1	1	3	3		
TNFRSF11A			1	1	1	1		
UNC80			1	1	1	1		
ZFHX4			1	1	2	2		
ARID1A							1	2
CARD11	1	1						
CLSTN1							1	1
CXCR4							1	1
DYNC2H1			2	2				
ERAP2					2	2		
FASN	1	1						
GSTP1							1	1
HDAC7					1	1		
ID3	1	1						
IGLL5	1	1						
KLHL7	1	1						
KDM6A			1	1				
KMT2D							1	1
METAP2					1	1		
MYC			1	1				
MYH4					1	1		
PTPN21					1	1		
SALL3			1	1				
TBC1D4			1	1				
TET1	1	1						
TP53	1	1						
XPC							1	1
KMT2B			1					
MAP2	1							

The Arabic numeral indicates the number of mutations which were found in each gene for each sample type.

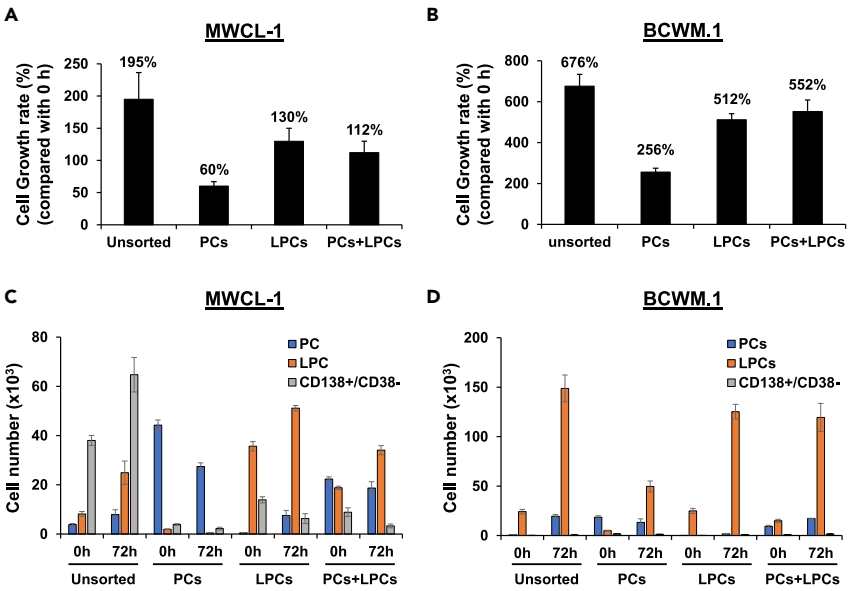

Figure 3. The growth rate of PCs and LPCs isolated from WM cell lines

Unsorted cells, PCs alone, LPCs alone, and PCs with LPCs FACs-sorted from WM cell lines were seeded into 9-well plates at the same density. After 72 h, PCs, LPCs, and $CD138^{-}/CD38^{+}$ cells were sorted using flow cytometer and cell number was counted using 123count eBeads. Cell growth rate in MWCL-1 (A) and BCWM.1 (B). The absolute cell number of each fraction was shown in (C) MWCL-1 and (D) BCWM.1. The representative data are shown from two individual experiments. Data are presented as mean ± S.D.

populations from BCWM.1 cell lines and patient 3, suggesting that MWCL-1 and patient 4 may have reduced response to rituximab.

PCs do not proliferate in culture and are differentiated from LPCs

To examine how the PCs and the LPCs potentially contribute to cell proliferation and pathogenesis in WM, we cultured PCs, LPC, PCs plus LPCs, and unsorted cells for 72 h.

The number of PCs (isolated from MWCL-1) decreased by 40% after 72 h of cell culture, consistent with the non-proliferative phenotype of PCs. Conversely, LPCs alone or co-cultures of PCs and LPCs (isolated from MWCL-1) both displayed moderate proliferation after 72 h of cell culture (130% and 112% of the initial population, respectively) whereas the unsorted population increased by 195.1% over the same period (Figure 3A).

The number of PCs (isolated from BCWM.1) increased by 256% of the initial population despite the non-proliferative feature of PCs (Figure 3B). Cell cultures of LPCs, co-cultures of PCs and LPCs (isolated from BCWM.1), and the unsorted population each proliferated by more than 500% of their respective initial population after 72 h of culture (Figure 3B).

We investigated the absolute cell number of each cell population at 72 h to determine which cell population proliferates and differentiates after 72 h in culture. In the unsorted MWCL-1 cells, the absolute cell number of all three populations, PCs, LPCs, and $CD138^{+}/CD38^{-}$ increased (Figure 3C). When PCs were cultured alone, the absolute cell number of three populations was decreased. When LPCs were cultured alone, the number of PCs and LPCs increased and $CD138^{+}/CD38^{-}$ cells decreased. When PCs and LPCs were co-cultured, PCs and $CD138^{+}/CD38^{-}$ cells decreased, and LPCs increased. These results suggest that LPCs and $CD138^{+}/CD38^{-}$ cells proliferate without any stimuli and differentiate to PCs. PCs did not proliferate because PCs decreased in absence of LPCs and $CD138^{+}/CD38^{-}$ cells (Figure 3C).

In unsorted BCWM.1 cells, the cell number of all three populations, PCs, LPCs, and $CD138^{+}/CD38^{-}$ cells increased (Figure 3D). In PCs alone, PCs decreased to 71% and LPCs increased 10-fold due to a small amount contamination during sorting. The proliferation of LPCs overcome the cell death of PCs and

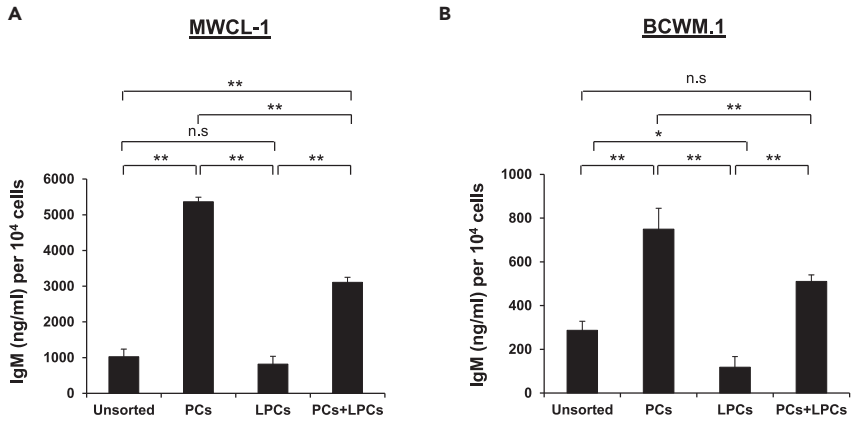

C

WM case	IgM PP	PCs	LPCs
Patient 1	2.1 g/L	0.82 %	7.52 %
Patient 2	16 g/L	3.43 %	2.64 %
Patient 3	23 g/L	16.28 %	4.98 %

Figure 4. IgM production in PCs and LPCs isolated from WM cell lines

After FACS sorting, each fraction of WM cell lines was cultured for 72 h without stimuli and supernatant was collected after 72 h for IgM ELISA.

(A) MWCL-1 and (B) BCWM.1. *p* values were calculated using one-way ANOVA (*$p < 0.05$; **$p < 0.01$; n.s; not significant). We performed two individual experiments and the representative data are shown. Data are presented as mean ± S.D.

(C) The amount of IgM paraprotein (IgM PP) of patients with WM was examined in the blood samples and the portion of PCs and LPCs was determined using flow cytometer.

resulted in the increase of cell number in PCs alone culture (Figure 3B), because of the fast growth rate of BCWM.1 cells. In LPCs alone and PCs plus LPCs, the cell number of all three populations increased and these results suggest that the proliferation rate of LPCs in BCWM.1 may overcome the cell death of PCs in all four cell culture conditions, unsorted, PCs alone, LPCs alone, and PCs plus LPCs. Overall, PCs have poor proliferative capacity and tend to decrease in culture without the support of LPCs or CD138+/CD38-cells.

PCs are responsible for the production of IgM

Secretion of IgM from each cell population was determined after 72 h of culture. In MWCL-1 cells, we found that the PCs population produced the largest amount of IgM (5362 ng/mL per 10^4 cells on average) (Figures 3A and 4A). IgM production in unsorted, LPCs, and PCs plus LPCs was on average, 1026, 818, and 3108 ng/mL per 10^4 cells, respectively. The amount of IgM production is correlated with PC number at 72 h showing Pearson's correlation coefficient (r) of 0.997 between IgM amount and the number of PCs (Figures 3C and 4A. In BCWM.1 cells, PCs produced the largest amount of IgM (749 ng/mL per 10^4 cells on average). IgM productions in unsorted, LPCs, and PCs plus LPCs were 286, 118, and 296 ng/mL per 10^4 cells, respectively (Figure 4B). Next, we compared the amount of IgM paraprotein in blood and the number of PCs in patients with WM, which were analyzed using flow cytometry (Figure 1B). We found the amount of IgM paraprotein is correlated with the percentage of PCs in BM samples with a Pearson's correlation coefficient (r) of 0.8506 (Figure 4C). These results suggest that PCs are a major IgM producer in WM cell lines and by extrapolation, in patients, and that targeting PCs could be therapeutically beneficial in deepening responses in patients with WM.

DISCUSSION

This study aimed to comprehensively characterize PCs which are postulated to play an important role in WM using immunophenotyping, MYD88 analysis, SNP microarray and next-generation sequencing; cell culture and quantification of IgM production to determine the secretory function of PCs relative to LPCs.

MYD88 L265P is the most common somatic mutation in patients with WM occurring in nearly 90% of cases (Treon et al., 2012). To demonstrate that the PCs are clonally related to LPCs, we performed MYD88 mutation analysis. MYD88 L265P was detected in both PC and LPC populations of the WM cell lines as well as one of the two patient samples tested. The other patient was negative for MYD88 L265P and did not demonstrate the mutation in either PCs or LPCs. This result suggests that the MYD88 L265P mutation, when present, co-exists in the PCs derived from WM samples. The demonstration of heterozygous MYD88 L265P mutation on NGS in both populations of two cell lines and one of the two patients further points toward a similar clonal origin. This also potentially explains the similar rate of MYD88 L265P mutation detection in CD19-sorted or unsorted populations in earlier studies (Varettoni et al., 2017; Gustine et al., 2017a). Additionally, the analysis of IGHV sequences of WM cells can provide information about tumor cell origin and antigen dependence since IGHV3 gene rearrangements have been demonstrated in 77% of patients with WM with intermediate to high mutation rates (Gachard et al., 2013). In MWCL-1 cell line, both PCs and LPCs showed IGHV3-15*01 while in BCWM-1, both expressed IGHV3-23*01. These findings suggest that PCs are likely derived from differentiation of malignant LPCs in WM.

The low mitotic index of plasma cells limits the utility of cytogenetic studies; however, fluorescent *in situ* hybridization or SNP microarray can be used to overcome this limitation (Cigudosa et al., 1998). In our study, there were no differences in SNP microarray identified between PCs and LPCs from either of the two cell lines or five of six patient samples examined (patients 2–6). However, patient 1 had a loss of 9p13.2 in the LPCs but not in the PCs. Deletion of the long arm of chromosome 6 is the most frequent cytogenetic abnormality seen in WM with a frequency of 38%–54% and is associated with adverse clinical and biological features along with deletion of 11q and trisomy 4 (Hunter et al., 2014; Nguỷen-Khac et al., 2013; Chang et al., 2009). Trisomy 18 (15%), 13q deletions (13%), 17p (TP53) deletions (8%), and trisomy 4 (8%) are some of the other aberrations seen (Nguyen-Khac et al., 2013). Deletions in the long arm of chromosome 6 (6q) involve genes that affect NF-kB including TNFAIP3 and HIVEP2, genes relating to apoptosis such as FOXO3, the BCL2 family of proteins (BCLAF1), and BTK (IBTK). The impact of 6q deletions on these genes remains to be elucidated. A 108MB deletion of 6q11.1-q27 was detected in <10% of both PC and LPC populations of MWCL-1. It was not detected in BCWM.1.

Of the six patients with WM evaluated using SNP microarray, only two showed chromosomal abnormalities. Patient 1 had 49MB AOH in 3p26.3-p21.31 in 60%–70% of both PCs and LPCs along with differential copy number loss of 1.42MB in 9p13.2 in LPCs alone. Deletions of chromosome 9p has not been previously demonstrated in WM as a recurrent abnormality; however, t(9; 14) which juxtaposes PAX5 and IgH has been reported in WM but is not specific to this disease, being present in other low-grade lymphomas showing plasmacytic differentiation (George et al., 2005). One patient (patient 4) showed two regions of AOH, the first, a 14.6MB in 6q13-q15 and the second, 17.9MB in 7q31.1–32.3 along with a 562KB copy number loss of 22q11.22 in 100% of both populations, suggestive of a germline change. Another gene at this locus is RNF38 which plays a role in oncogenesis and has potential association with colonic adenocarcinomas but has no established role in lymphomagenesis. Thus, the significance of our finding remains uncertain at this stage but could be explored further in a larger number of samples to demonstrate differential loss in LPCs compared to PCs. Otherwise, no differences in microarray findings were noted in the cellular fractions of the WM cell lines or the other patient samples.

Activating CXCR4 mutations (G protein-coupled chemokine receptor) are found in nearly one-third of patients with WM and more than 30 different types of nonsense and frameshift mutations in CXCR4 have been described with the most common variant being the C-terminus truncated mutation S338X (Hunter et al., 2014; Poulain et al., 2016). Pre-clinical studies have demonstrated enhanced and sustained AKT and ERK signaling leading to increased cell migration, adhesion, and survival of WM cells (Cao et al., 2015). Moreover, the presence of CXCR4 mutation in MYD88-mutated patients with WM on Ibrutinib is predictive of slower responses and low response rates (Treon et al., 2015). CXCR4 S338X mutation was found in both populations of one of the clinical samples and this patient showed high level (>90%) BM involvement and consequent cytopenias compared to the other patient not showing this mutation. These results are consistent with previous reports suggesting that patients with both MYD88 and truncated CXCR4 mutations have high BM LPC involvement and are more symptomatic (Chang et al., 2009; Treon et al., 2014; Schmidt et al., 2015; Cao et al., 2017).

KMT2D mutations were observed in 24% of patients with WM in one study using NGS (Cigudosa et al., 1998). Other less common recurrent somatic abnormalities in WM include ARID1A (17%), CD79B (8%–15%), TP53 (10%), PRDM1 (6%), NOTCH2 (5%), and TRAF3.7,11 The frameshift mutation on ARID1A

was detected in both cell populations of patient 2. NOTCH2 mutation was found in all samples except LPCs in BCWM.1 cell line. Altered NOTCH pathway signaling in lymphomas is associated with shorter PFS (Progression-free survival) and OS (Overall survival).

Other mutations which have been previously described in WM include PRDM2 and SYNE1. PRDM2 gene mutation was noted in both populations in two WM cell lines and one clinical sample while the other patient sample only had this mutation in the $CD19^{+}$ population.

Novel mutations that have not been previously reported in WM but noted in our analysis include ALK, ATM, IKZF3, LONP1, MKI67, MTHER, MTRR, OBSCN, PLEKHG1, SYNE1, TET2, TNFRSF11a, UNC80, and ZFHX4. Some of these mutations have a well-known association with lymphomagenesis and solid organ malignancies. Of these, ALK, ATM, and TET2 have prognostic relevance—ALK mutation in anaplastic lymphoma being associated with favorable prognosis while ATM and TET2 confers adverse prognosis and shorter PFS in some lymphoid malignancies (Choi et al., 2016; Lemonnier et al., 2012). Mutations in FCGR3A were detected in all patients and polymorphisms within this gene have been associated with a favorable response to rituximab-based therapy (Treon et al., 2011). In summary, our mutational profiling indicates a similar clonal origin for both the LPC and PC in WM. Additionally, we have found some novel mutations not previously described in WM some of which may have prognostic relevance. However, the small number of clinical samples and the lack of clinical information (relapsed/refractory status and their prior treatments) which may affect the mutational profile due to clonal evolution is a limitation of this study which precludes definitive conclusions. The demonstration of newer mutations not previously seen in patients with WM may be further studied in a larger patient cohort to determine if these are recurring mutations as some of these may have prognostic significance or may even be potentially targetable.

In MWCL1 cell line, the increase of PCs in the unsorted population is due to the simultaneous differentiation of LPCs because PCs are non-proliferative by itself. The decrease of LPCs and $CD138^{+}/CD38^{-}$ cells in the PCs alone population is due to differentiation into PCs and the proliferation of LPCs and $CD138^{+}/CD38^{-}$ cells did not overcome the rate of differentiation to PCs in this population (Figures 3A and 3C). In BCWM.1, the increase of PCs alone is the result of the differentiation of LPCs and $CD138^{+}/CD38^{-}$ cells as result of minor contamination during sorting, and the increase of LPCs is the result of proliferation (Figures 3B and 3D).

Our final objective was to determine which cellular fraction was responsible for IgM hypersecretion for which isolated PCs and LPCs from both cell lines were cultured for 72 h with culture media analyzed for IgM secretion. We found that unstimulated culture studies performed on the unsorted and LPCs alone demonstrated increase in the number of PCs (using CD138+/CD38+ enumeration) after 72 h in both cell lines supporting the long-held hypothesis of spontaneous differentiation (Figure 3). Subsequent determination of IgM secretion by ELISA confirmed the predominant role of PCs in its production as evidenced by the high IgM levels generated by PCs alone while smaller amounts noted from the LPC fraction is likely produced by the newly differentiated PCs. We also determined that the IgM production is correlated with PCs percentage in patients with WM (Figure 4).

PCs can initiate the development of various malignancies, including multiple myeloma (Pal Singh et al., 2018). Therefore, therapeutic targeting of key molecules that drive differentiation and proliferation of PCs could improve the treatment outcome in malignancies driven by PCs. For instance, Bruton's tyrosine kinase (BTK) plays a critical role in the proliferation and survival of PCs (Pal Singh et al., 2018). Therefore, inhibitors of BTK are promising treatment options not only in WM but also in malignancies such as multiple myeloma (Hendriks et al., 2014; Von Suskil et al., 2021). From a clinical perspective, this study has a potentially important implication for therapy. As we have shown for the first time, using cell culture techniques that the PC compartment is the major producer of IgM protein, there may be a role for targeting PCs to deepen responses. In summary, our findings also confirm the common derived hypothesis that PCs in WM are formed by differentiation of LPCs and hence are clonally related.

Limitations of this study

In this study, we used two WM cell lines (MWCL-1 and BCWM.1), and primary cells from patients with WM to characterize the molecular genetics and secretory function of PCs. However, experiments performed using cell lines may not mimic the complex biological processes *in vivo*. Furthermore, our study used a small number of patients, limiting us to draw firm conclusions regarding chromosomal copy number changes

in patients with WM. Therefore, future studies using a larger cohort of patients with WM could provide further insights into the genetic and secretory function of PCs.

STAR★METHODS

Detailed methods are provided in the online version of this paper and include the following:

- KEY RESOURCES TABLE
- RESOURCE AVAILABILITY
  - Lead contact
  - Materials availability
  - Data and code availability
- EXPERIMENTAL MODEL AND SUBJECT DETAILS
  - Cell lines and tissue culture
  - Human study oversight
- METHOD DETAILS
  - Cell line culture
  - Cell sorting to isolate plasma cell and lymphoplasmacytic cell subpopulations
  - Flow cytometry sorting
  - Magnetic-activated cell sorting (MACS)
  - Genomic DNA extraction
  - Mutational analysis of *Myd88* and IgHV isotyping
  - DNA single nucleotide polymorphism (SNP) microarray
  - Next generation sequencing
  - Determination of cell growth rate in each cell fractions from WM cell lines
  - ELISA
- QUANTIFICATION AND STATISTICAL ANALYSIS
  - Statistical analysis

SUPPLEMENTAL INFORMATION

Supplemental information can be found online at https://doi.org/10.1016/j.isci.2022.104856.

ACKNOWLEDGMENTS

We acknowledge the support of Ali El-Ayoubi with flow cytometric analysis of clinical samples, and of Dr. M. Gohar Maqbool for providing additional clinical comments on the study. We acknowledge the scientific and technical assistance from the Flow Cytometry Facility of The John Curtin School of Medical Research, ANU. We would like to thank the ACT Haematology Research Tissue Bank for providing patient samples and the Private Practice Trust Fund, Canberra Hospital, for providing funding for this project.

AUTHOR CONTRIBUTIONS

All of the authors discussed the results and contributed to the final manuscript. Study conception and design: J.L., J.Q.W., K.S., D.T.; acquisition of data: J.L., F.W.; analysis and interpretation of data: J.L.; drafting of manuscript: J.L., D.E.T., A.P., S.M., D.T.

DECLARATION OF INTERESTS

The authors declare no competing interests relevant to this manuscript. DT has received research funding from Janssen and Roche, and honoraria from CSL, Takeda, Roche, Janssen, Beigene, and EUSA.

INCLUSION AND DIVERSITY

One or more of the authors of this paper self-identifies as an underrepresented ethnic minority in science. The author team identifies as being diverse and multi-ethnic. Both the first and last authors are women.

Received: May 5, 2022
Revised: June 16, 2022
Accepted: July 25, 2022
Published: August 19, 2022

REFERENCES

Calame, K.L. (2001). Plasma cells: finding new light at the end of B cell development. Nat. Immunol. *2*, 1103–1108.

Cao, X.X., Meng, Q., Cai, H., He, T.H., Zhang, C.L., Su, W., Sun, J., Li, Y., Xu, W., Zhou, D.B., and Li, J. (2017). Detection of MYD88 L265P and WHIM-like CXCR4 mutation in patients with IgM monoclonal gammopathy related disease. Ann. Hematol. *96*, 971–976.

Cao, Y., Hunter, Z.R., Liu, X., Xu, L., Yang, G., Chen, J., Patterson, C.J., Tsakmaklis, N., Kanan, S., Rodig, S., et al. (2015). The WHIM-like CXCR4(S338X) somatic mutation activates AKT and ERK, and promotes resistance to ibrutinib and other agents used in the treatment of Waldenstrom's Macroglobulinemia. Leukemia *29*, 169–176.

Chang, H., Qi, C., Trieu, Y., Jiang, A., Young, K.H., Chesney, A., Jani, P., Wang, C., Reece, D., and Chen, C. (2009). Prognostic relevance of 6q deletion in Waldenstrom's macroglobulinemia: a multicenter study. Clin. Lymphoma Myeloma *9*, 36–38.

Choi, M., Kipps, T., and Kurzrock, R. (2016). ATM mutations in cancer: therapeutic implications. Mol. Cancer Ther. *15*, 1781–1791.

Cigudosa, J.C., Rao, P.H., Calasanz, M.J., Odero, M.D., Michaeli, J., Jhanwar, S.C., and Chaganti, R.S. (1998). Characterization of nonrandom chromosomal gains and losses in multiple myeloma by comparative genomic hybridization. Blood *91*, 3007–3010.

De Tute, R.M., Rawstron, A.C., and Owen, R.G. (2013). Immunoglobulin M concentration in Waldenstrom macroglobulinemia: correlation with bone marrow B cells and plasma cells. Clin. Lymphoma Myeloma Leuk. *13*, 211–213.

Dunne, A., Ejdeback, M., Ludidi, P.L., O'Neill, L.A.J., and Gay, N.J. (2003). Structural complementarity of Toll/interleukin-1 receptor domains in Toll-like receptors and the adaptors Mal and MyD88. J. Biol. Chem. *278*, 41443–41451.

El-Ayoubi, A., Wang, J.Q., Hein, N., and Talaulikar, D. (2017). Role of plasma cells in Waldenstrom macroglobulinaemia. Pathology *49*, 337–345.

Fahey, J.L., Barth, W.F., and Solomon, A. (1965). Serum hyperviscosity syndrome. JAMA *192*, 464–467.

Gachard, N., Parrens, M., Soubeyran, I., Petit, B., Marfak, A., Rizzo, D., Devesa, M., Delage-Corre, M., Coste, V., Laforêt, M.P., et al. (2013). IGHV gene features and MYD88 L265P mutation separate the three marginal zone lymphoma entities and Waldenstrom macroglobulinemia/ lymphoplasmacytic lymphomas. Leukemia *27*, 183–189.

George, T.I., Wrede, J.E., Bangs, C.D., Cherry, A.M., Warnke, R.A., and Arber, D.A. (2005). Low-grade B-Cell lymphomas with plasmacytic differentiation lack PAX5 gene rearrangements. J. Mol. Diagn. *7*, 346–351.

Guan, B., Wang, T.L., and Shih, I.M. (2011). ARID1A, a factor that promotes formation of SWI/SNF-mediated chromatin remodeling, is a tumor suppressor in gynecologic cancers. Cancer Res. *71*, 6718–6727.

Gustine, J.N., Meid, K., Dubeau, T., Hunter, Z.R., Xu, L., Yang, G., Ghobrial, I.M., Treon, S.P., and Castillo, J.J. (2017b). Serum IgM level as predictor of symptomatic hyperviscosity in patients with Waldenstrom macroglobulinaemia. Br. J. Haematol. *177*, 717–725.

Gustine, J., Meid, K., Xu, L., Hunter, Z.R., Castillo, J.J., and Treon, S.P. (2017a). To select or not to select? The role of B-cell selection in determining the MYD88 mutation status in Waldenstrom Macroglobulinaemia. Br. J. Haematol. *176*, 822–824.

Hendriks, R.W., Yuvaraj, S., and Kil, L.P. (2014). Targeting Bruton's tyrosine kinase in B cell malignancies. Nat. Rev. Cancer *14*, 219–232.

Hodge, L.S., Novak, A.J., Grote, D.M., Braggio, E., Ketterling, R.P., Manske, M.K., Price Troska, T.L., Ziesmer, S.C., Fonseca, R., Witzig, T.E., et al. (2011). Establishment and characterization of a novel Waldenstrom macroglobulinemia cell line, MWCL-1. Blood *117*, e190–e197.

Howard, M.T., Hodnefield, J., and Morice, W.G. (2011). Immunohistochemical phenotyping of plasma cells in lymphoplasmacytic lymphoma/ Waldenstrom's macroglobulinemia is comparable to flow cytometric techniques. Clin. Lymphoma Myeloma Leuk. *11*, 96–98.

Hunter, Z.R., Xu, L., Yang, G., Zhou, Y., Liu, X., Cao, Y., Manning, R.J., Tripsas, C., Patterson, C.J., Sheehy, P., and Treon, S.P. (2014). The genomic landscape of Waldenstrom macroglobulinemia is characterized by highly recurring MYD88 and WHIM-like CXCR4 mutations, and small somatic deletions associated with B-cell lymphomagenesis. Blood *123*, 1637–1646.

Koene, H.R., Kleijer, M., Algra, J., Roos, D., Von Dem Borne, A.E., and De Haas, M. (1997). Fc gammaRIIIa-158V/F polymorphism influences the binding of IgG by natural killer cell Fc gammaRIIIa, independently of the Fc gammaRIIIa-48L/R/H phenotype. Blood *90*, 1109–1114.

Lacy, S.E., Barrans, S.L., Beer, P.A., Painter, D., Smith, A.G., Roman, E., Cooke, S.L., Ruiz, C., Glover, P., Van Hoppe, S.J.L., et al. (2020). Targeted sequencing in DLBCL, molecular subtypes, and outcomes: a Haematological Malignancy Research Network report. Blood *135*, 1759–1771.

Lemonnier, F., Couronné, L., Parrens, M., Jaïs, J.P., Travert, M., Lamant, L., Tournillac, O., Rousset, T., Fabiani, B., Cairns, R.A., et al. (2012). Recurrent TET2 mutations in peripheral T-cell lymphomas correlate with TFH-like features and adverse clinical parameters. Blood *120*, 1466–1469.

Lin, P., Hao, S., Handy, B.C., Bueso-Ramos, C.E., and Medeiros, L.J. (2005). Lymphoid neoplasms associated with IgM paraprotein: a study of 382 patients. Am. J. Clin. Pathol. *123*, 200–205.

Lin, S.C., Lo, Y.C., and Wu, H. (2010). Helical assembly in the MyD88-IRAK4-IRAK2 complex in TLR/IL-1R signalling. Nature *465*, 885–890.

Lynch, R.C., Gratzinger, D., and Advani, R.H. (2017). Clinical impact of the 2016 update to the WHO lymphoma classification. Curr. Treat. Options Oncol. *18*, 45.

Mehta, J., and Singhal, S. (2003). Hyperviscosity syndrome in plasma cell dyscrasias. Semin. Thromb. Hemost. *29*, 467–471.

Morice, W.G., Chen, D., Kurtin, P.J., Hanson, C.A., and Mcphail, E.D. (2009). Novel immunophenotypic features of marrow lymphoplasmacytic lymphoma and correlation with Waldenstrom's macroglobulinemia. Mod. Pathol. *22*, 807–816.

Morice, W.G., Hanson, C.A., Kumar, S., Frederick, L.A., Lesnick, C.E., and Greipp, P.R. (2007). Novel multi-parameter flow cytometry sensitively detects phenotypically distinct plasma cell subsets in plasma cell proliferative disorders. Leukemia *21*, 2043–2046.

Morin, R.D., Mungall, K., Pleasance, E., Mungall, A.J., Goya, R., Huff, R.D., Scott, D.W., Ding, J., Roth, A., Chiu, R., et al. (2013). Mutational and structural analysis of diffuse large B-cell lymphoma using whole-genome sequencing. Blood *122*, 1256–1265.

Muzio, M., Ni, J., Feng, P., and Dixit, V.M. (1997). IRAK (Pelle) family member IRAK-2 and MyD88 as proximal mediators of IL-1 signaling. Science *278*, 1612–1615.

Ngo, V.N., Young, R.M., Schmitz, R., Jhavar, S., Xiao, W., Lim, K.H., Kohlhammer, H., Xu, W., Yang, Y., Zhao, H., et al. (2011). Oncogenically active MYD88 mutations in human lymphoma. Nature *470*, 115–119.

Nguyen-Khac, F., Lambert, J., Chapiro, E., Grelier, A., Mould, S., Barin, C., Daudignon, A., Gachard, N., Struski, S., Henry, C., et al. (2013). chromosomal aberrations and their prognostic value in a series of 174 untreated patients with waldenstrom's macroglobulinemia. Haematologica *98*, 649–654.

Owen, R.G., Treon, S.P., Al-Katib, A., Fonseca, R., Greipp, P.R., Mcmaster, M.L., Morra, E., Pangalis, G.A., San Miguel, J.F., Branagan, A.R., and Dimopoulos, M.A. (2003). Clinicopathological definition of Waldenstrom's macroglobulinemia: consensus panel recommendations from the Second International Workshop on Waldenstrom's Macroglobulinemia. Semin. Oncol. *30*, 110–115.

Pal Singh, S., Dammeijer, F., and Hendriks, R.W. (2018). Role of Bruton's tyrosine kinase in B cells and malignancies. Mol. Cancer *17*, 57.

Pasqualucci, L., Trifonov, V., Fabbri, G., Ma, J., Rossi, D., Chiarenza, A., Wells, V.A., Grunn, A., Messina, M., Elliot, O., et al. (2011). Analysis of the coding genome of diffuse large B-cell lymphoma. Nat. Genet. *43*, 830–837.

Pasricha, S.R., Juneja, S.K., Westerman, D.A., and Came, N.A. (2011). Bone-marrow plasma cell burden correlates with IgM paraprotein concentration in Waldenstrom macroglobulinaemia. J. Clin. Pathol. *64*, 520–523.

Peceliunas, V., Janiulioniene, A., Matuzeviciene, R., and Griskevicius, L. (2011). Six color flow

cytometry detects plasma cells expressing aberrant immunophenotype in bone marrow of healthy donors. Cytometry B Clin. Cytom. *80*, 318–323.

Phelan, J.D., Young, R.M., Webster, D.E., Roulland, S., Wright, G.W., Kasbekar, M., Shaffer, A.L., 3rd, Ceribelli, M., Wang, J.Q., Schmitz, R., et al. (2018). A multiprotein supercomplex controlling oncogenic signalling in lymphoma. Nature *560*, 387–391.

Poulain, S., Roumier, C., Venet-Caillault, A., Figeac, M., Herbaux, C., Marot, G., Doye, E., Bertrand, E., Geffroy, S., Lepretre, F., et al. (2016). Genomic landscape of CXCR4 mutations in waldenstrom macroglobulinemia. Clin. Cancer Res. *22*, 1480–1488.

Schmidt, J., Federmann, B., Schindler, N., Steinhilber, J., Bonzheim, I., Fend, F., and Quintanilla-Martinez, L. (2015). MYD88 L265P and CXCR4 mutations in lymphoplasmacytic lymphoma identify cases with high disease activity. Br. J. Haematol. *169*, 795–803.

Schmitz, R., Wright, G.W., Huang, D.W., Johnson, C.A., Phelan, J.D., Wang, J.Q., Roulland, S., Kasbekar, M., Young, R.M., Shaffer, A.L., et al. (2018). Genetics and pathogenesis of diffuse large B-cell lymphoma. N. Engl. J. Med. *378*, 1396–1407.

Soh, K.T., Tario, J.D., Jr., Hahn, T., Hillengass, J., Mccarthy, P.L., and Wallace, P.K. (2021). CD319 (SLAMF7) an alternative marker for detecting plasma cells in the presence of daratumumab or elotuzumab. Cytometry B Clin. Cytom. *100*, 497–508.

Stone, M.J., and Bogen, S.A. (2012). Evidence-based focused review of management of hyperviscosity syndrome. Blood *119*, 2205–2208.

Treon, S.P., Cao, Y., Xu, L., Yang, G., Liu, X., and Hunter, Z.R. (2014). Somatic mutations in MYD88 and CXCR4 are determinants of clinical presentation and overall survival in Waldenstrom macroglobulinemia. Blood *123*, 2791–2796.

Treon, S.P., Xu, L., and Hunter, Z. (2015). MYD88 mutations and response to ibrutinib in waldenstrom's macroglobulinemia. N. Engl. J. Med. *373*, 584–586.

Treon, S.P., Xu, L., Yang, G., Zhou, Y., Liu, X., Cao, Y., Sheehy, P., Manning, R.J., Patterson, C.J., Tripsas, C., et al. (2012). MYD88 L265P somatic mutation in Waldenstrom's macroglobulinemia. N. Engl. J. Med. *367*, 826–833.

Treon, S.P., Yang, G., Hanzis, C., Ioakimidis, L., Verselis, S.J., Fox, E.A., Xu, L., Hunter, Z.R., Tseng, H., Manning, R.J., et al. (2011). Attainment of complete/very good partial response following rituximab-based therapy is an important determinant to progression-free survival, and is impacted by polymorphisms in FCGR3A in Waldenstrom macroglobulinaemia. Br. J. Haematol. *154*, 223–228.

Van Dongen, J.J., Langerak, A.W., Brüggemann, M., Evans, P.A.S., Hummel, M., Lavender, F.L., Delabesse, E., Davi, F., Schuuring, E., García-Sanz, R., et al. (2003). Design and standardization of PCR primers and protocols for detection of clonal immunoglobulin and T-cell receptor gene recombinations in suspect lymphoproliferations: report of the BIOMED-2 Concerted Action BMH4-CT98-3936. Leukemia *17*, 2257–2317.

Varettoni, M., Arcaini, L., Zibellini, S., Boveri, E., Rattotti, S., Riboni, R., Corso, A., Orlandi, E., Bonfichi, M., Gotti, M., et al. (2013). Prevalence and clinical significance of the MYD88 (L265P) somatic mutation in Waldenstrom's macroglobulinemia and related lymphoid neoplasms. Blood *121*, 2522–2528.

Varettoni, M., Zibellini, S., Defrancesco, I., Ferretti, V.V., Rizzo, E., Malcovati, L., Gallì, A., Porta, M.G.D., Boveri, E., Arcaini, L., et al. (2017). Pattern of somatic mutations in patients with Waldenstrom macroglobulinemia or IgM monoclonal gammopathy of undetermined significance. Haematologica *102*, 2077–2085.

Von Suskil, M., Sultana, K.N., Elbezanti, W.O., Al-Odat, O.S., Chitren, R., Tiwari, A.K., Challagundla, K.B., Srivastava, S.K., Jonnalagadda, S.C., Budak-Alpdogan, T., and Pandey, M.K. (2021). Bruton's tyrosine kinase targeting in multiple myeloma. Int. J. Mol. Sci. *22*, 5707.

Wada, N., Ikeda, J.I., Nojima, S., Tahara, S.I., Ohshima, K., Okuzaki, D., and Morii, E. (2016). Requirement of CXCL12-CXCR7 signaling for CD20(-) CD138(-) double-negative population in lymphoplasmacytic lymphoma. Lab. Invest. *96*, 517–525.

Weng, W.K., and Levy, R. (2003). Two immunoglobulin G fragment C receptor polymorphisms independently predict response to rituximab in patients with follicular lymphoma. J. Clin. Oncol. *21*, 3940–3947.

Xu, L., Hunter, Z.R., Yang, G., Cao, Y., Liu, X., Manning, R., Tripsas, C., Chen, J., Patterson, C.J., Kluk, M., et al. (2014). Detection of MYD88 L265P in peripheral blood of patients with Waldenstrom's Macroglobulinemia and IgM monoclonal gammopathy of undetermined significance. Leukemia *28*, 1698–1704.

Xu, L., Hunter, Z.R., Yang, G., Zhou, Y., Cao, Y., Liu, X., Morra, E., Trojani, A., Greco, A., Arcaini, L., et al. (2013). MYD88 L265P in Waldenstrom macroglobulinemia, immunoglobulin M monoclonal gammopathy, and other B-cell lymphoproliferative disorders using conventional and quantitative allele-specific polymerase chain reaction. Blood *121*, 2051–2058.

STAR★METHODS

KEY RESOURCES TABLE

REAGENT or RESOURCE	SOURCE	IDENTIFIER
Antibodies		
Alexa 647-CD319	BD Biosciences	#564338; RRID:AB_2738754
APC-CD138	DAKO	#C7256; RRID:N/A
APC-H7-CD19	BD Biosciences	#560177; RRID:AB_1645470
BV421-CD38	BD Biosciences	#562444; RRID:AB_11151894
PerCP-CD20	BD Biosciences	#347674; RRID:AB_400339
V500-CD45	BD Biosciences	#560777; RRID:AB_1937324
Fixable viability stain 700	BD Biosciences	564997; RRID:AB_2869637
CD138 microbeads	Miltenyl Biotec	#130-111-744
CD19 microbeads	Miltenyl Biotec	#130-050-301
Chemicals, peptides, and recombinant proteins		
AutoMACS running buffer & elution buffer	Miltenyl Biotec	#130-091-211
MyTaq HS DNA polymerase	BIOLINE	#BIO-21111
GelRed	Biotium	#41003
123 count eBeads	Affymetrix	#01-1234
Critical commercial assays		
Qubit dsDNA BR assay kit	Molecular probes	#Q32850
Whole blood column kit	Miltenyl Biotec	#130-093-545
QIAamp DNA mini kit	QIAGEN	#51304
QIAquick gel extraction kit	QIAGEN	#28704
High sensitivity DNA kit	Agilent Technologies	#5067-4626
SureSelectXT Low Input Target Enrichment System	Agilent Technologies	#G9707B
Human IgM ELISA kit	Abcam	#ab137982
Oligonucleotides		
Biomed-2 IGHv-specific primers FR3	(Van Dongen et al., 2003)	PMID: 14671650
V_H1: TGGAGCTGAGCAGCCTGAGATCTGA	(Van Dongen et al., 2003)	PMID: 14671650
V_H2: CAATGACCAACATGGACCCTGTGGA	(Van Dongen et al., 2003)	PMID: 14671650
V_H3: TCTGCAAATGAACAGCCTGAGAGCC	(Van Dongen et al., 2003)	PMID: 14671650
V_H4: GAGCTCTGTGACCGCCGCGGACACG	(Van Dongen et al., 2003)	PMID: 14671650
V_H5: CAGCACCGCCTACCTGCAGTGGAGC	(Van Dongen et al., 2003)	PMID: 14671650
V_H6: GTTCTCCCTGCAGCTGAACTCTGTG	(Van Dongen et al., 2003)	PMID: 14671650
V_H7: CAGCACGGCATATCTGCAGATCAG	(Van Dongen et al., 2003)	PMID: 14671650
J_H: CCAGTGGCAGAGGAGTCCATTC	(Van Dongen et al., 2003)	PMID: 14671650
Myd88 F: AATGTGTGCCAGGGGTACTTG	(Xu et al., 2013)	PMID: 23321251
Myd88 R: GCCTTGTACTTGATGGGG	(Xu et al., 2013)	PMID: 23321251
Myd88 L265P R: CCTTGTACTTGATGGGGAACG	(Xu et al., 2013)	PMID: 23321251
Software and algorithms		
Flow Jo	BD Biosciences	https://www.flowjo.com
PRISM 9	GraphPad Software, Inc.	http://www.graphpad.com
Surecall 3.5 Mac	Agilent Technologies	https://www.agilent.com/search/?Ntt=surecell

RESOURCE AVAILABILITY

Lead contact

Further information and requests for resources and reagents should be directed to and will be fulfilled by the lead contact, Dipti Talaulikar (Dipti.Talaullikar@act.gov.au).

Materials availability

This study did not generate new unique reagents.

Data and code availability

The clinical data reported in this study cannot be deposited in a public repository because of privacy and ethical reasons. To request access, contact the lead contact at Dipti.Talaulikar@act.gov.au

This paper does not report original code.

Any additional information required to reanalyze the data reported in this paper is available from the lead contact upon request.

EXPERIMENTAL MODEL AND SUBJECT DETAILS

Cell lines and tissue culture

The human Waldenström macroglobulinemia (WM) cell lines, MWCL-1 and BCWM.1 were provided by the Ansell lab at the Mayo Clinic and the Treon lab at the Dana-Farber Cancer Institute respectively.

Human study oversight

Patient samples were obtained from the ACT Haematology Research Tissue Bank. Bone marrow (BM) aspirates were collected after informed consent from six WM patients (four males and two females) with a median age of 71 years (range 56 to 78 years) after informed written consent was obtained. The selected patients were based on availability of BM samples. All the experiments were conducted as per guidelines of the ACT Health Human Research Ethics Committee (ACTH-HREC) under the protocol number ETHLR.12.170.

METHOD DETAILS

Cell line culture

Both WM cell lines were maintained in RPMI1640 containing 10% heat-inactivated fetal bovine serum FBS (Sigma-Aldrich, USA) and 1× antibiotic-antimycotic (ThermoFisher, USA).

Cell sorting to isolate plasma cell and lymphoplasmacytic cell subpopulations

Flow cytometry sorting and magnetic-activated cell sorting (MACS) were used to sort cellular fractions from two WM cell lines and six WM patient samples. The sorted cellular fractions were applied for each experiment as summarised in Table S1.

Flow cytometry sorting

Both WM cell lines were pelleted by centrifugation at 300*g* and resuspended in PBS. A total of 5×10^5 cells were stained with fixable viability stain 700 at room temperature for 10 min in the dark and washed twice with PBS containing 2.5% FBS. Next, the cells were stained with the appropriate antibody combinations outlined in the Key resources table and Figure 1A and incubated at room temperature for 30 min in the dark. Cells were then washed twice in PBS containing 2.5% FBS and resuspended in a final volume of 200 μL PBS containing 1% FBS. The cells were then analysed by flow cytometry on a BD APF LSRII cytometer (BD Biosciences).

For cell sorting, a total of 5×10^7 cells were stained with the antibody panel described in the Key resources table and separated using the BD FACS Aria I cell sorter (BD Biosciences). Firstly, cells were displayed on a forward scatter (FSC-A) versus side scatter (SSC-A) plot to discriminate debris and aggregates with low forward scatter and high side scatter. Doublets were eliminated using a forward-scatter height (FSC-H) versus forward-scatter area (FSC-A) plot. The negative fraction was gated using flexible viability stain 700 for live cell fractions and the live cells were then evaluated for expression of the cell surface markers. Cell preparations stained with antibodies against all markers except one (fluorescence minus one controls, FMO)

were used to determine the gating boundary between positive and negative stained cells. For PCs, $CD45^{low}/CD138^{+}/CD38^{+}$ cells were selected and for LPCs, $CD45^{high}/CD138^{-}/CD19^{+}/CD20^{+}$ cells were selected (Morice et al., 2007; Peceliunas et al., 2011; Howard et al., 2011). The purity of sorted cells was ascertained by running an aliquot of sorted cells back on the sorter, after finishing the sort. Flow cytometric analysis and cell sorting was performed at the Flow Cytometry Facility at the John Curtin School of Medical Research, ANU. Data was analysed using FlowJo v10.

Magnetic-activated cell sorting (MACS)

Two cultured WM cell lines were sorted into $CD138^{+}$ (PCs) and then $CD19^{+}/CD138^{-}$ population (LPCs) using MACS Separator. This process was also applied to frozen BM from six WM patients. To elaborate, frozen BM aspirate was thawed using a 37 °C waterbath and then incubated with CD138 microbeads. The BM-bead mixture was filtered through a whole blood magnetic column where the magnetic beads attached to the $CD138^{+}$ PCs remain in the column and the $CD138^{-}$ cells pass through and are collected for subsequent CD19 enrichment. An elution buffer then releases the beads from the magnet and the $CD138^{+}$ eluate is collected. The $CD138^{-}$ cells were then incubated with CD19 microbeads and the cell-bead mixture was filtered through a whole blood magnetic column where the magnetic beads attached to the $CD19^{+}$ lymphocytes remain in the column. All other cell types passing through the filter were discarded. An elution buffer was then used to release the beads from the magnet and the $CD19^{+}$ eluate was collected. DNA extraction was performed on each eluted cell population using the QIAamp DNA mini kit (QIAGEN). The concentration of genomic DNA was quantified using a NanoDrop 2000 spectrophotometer (Thermo Scientific).

Genomic DNA extraction

Genomic DNA was extracted from PC and LPC populations from WM cell lines and WM patients using the QIAamp DNA mini kit following the manufacturers' instructions (QIAGEN). The concentration of genomic DNA from each of the cell populations was quantified using the Qubit dsDNA BR assay kit (Molecular probes).

Mutational analysis of *Myd88* and IgHV isotyping

Genomic DNA (20 ng) of each population was amplified with MyTaq HS DNA polymerase (BIOLINE) for 36 cycles in a T10 Thermal Cycler (BIO-RAD, USA): 95 °C for 15 s, 56 °C for 15 s, and 72 °C for 20 s. Primer sequences for *MYD88* were as follows: *Myd88* forward primer 5′-AATGTGTGCCAGGGGTACTTG-3′; *Myd88* reverse primer 5′-GCCTTGTACTTGATGGGG-3′; *Myd88* reverse primer for mutant (L265P) 5′-CCTTGT ACTTGATGGGGAACG-3′. Primers were designed and evaluated to produce a 159bp amplicon which allowed for the detection of the *Myd88* T>C substitution that encodes for the oncogenic MYD88 L265P variant (Xu et al., 2013). The immunoglobulin heavy chain (IgHV) was amplified with Biomed-2 specific primers for FR3 (Van Dongen et al., 2003). PCR products were analysed by 2% agarose gel electrophoresis. Gels were stained with GelRed (Biotium) and visualized using a Biorad ChemiDoc Touch imaging system. PCR products were excised from agarose gels and purified using the QIAquick gel extraction kit (QIAGEN), and then analysed by DNA Sanger sequencing performed at the Biomolecular Resource Facility (BRF) at the John Curtin School of Medical Research, ANU. Sequencing was analysed using NCBI IgBLAST tool.

DNA single nucleotide polymorphism (SNP) microarray

DNA extracted from PCs and LPCs (500 ng) from two cell lines and six patient samples was sent to a NATA accredited referral laboratory (Victorian Clinical Genetics Service, Department of Cytogenetics, The Royal Children's Hospital, for SNP microarray processing using the Illumina Infinium CoreExome SNP microarray. Data was returned from the referral laboratory via OwnCloud employing a secure login. SNP microarray variant call files and quality data were downloaded to the secure network in our organisation where they were accessed to be analysed using Karyostudio™ software.

Next generation sequencing

We designed a customized Capture Library targeting approximately 200 genes known to be related with tumorigenesis and lymphomagenesis (Morin et al., 2013; Lacy et al., 2020; Pasqualucci et al., 2011; Schmitz et al., 2018). The customized capture library was designed using SureDesign program and produced by Agilent. PCs and LPCs from both cell lines and two patient samples were used for this analysis.

Genomic DNA (50 ng) was fragmented to between 150 bp and 200 bp in size using a Covaris S220 sonicator (Covaris) and the quality and quantity of fragmented DNA was assessed using Bioanalyser High Sensitivity DNA kit (Agilent Technologies, USA). The NGS library was prepared according to manufacturer's manual for SureSelectXT Low Input Target Enrichment System for Illumina Paired-End Multiplexed Sequencing Library using Custom 0.5 - 2.9 Mb Capture library (Aqilent Technologies). The purified libraries were assessed using Bioanalyser High Sensitivity DNA kit and were sequenced on the Illumina NextSeq500 platform according to Illumina protocols, generating paired-end 100 bp reads. Somatic single-nucleotide variants (SNVs) were identified in genomes using Agilent SureCall version 4.0 to be aligned to the human reference genome (GRCh37/HG19). We considered variants to generate an amino acid change, including frame shift, by filtering against variant allele frequency according to 1000G using cut offs scores of <0.1. The variants were further filtered for two tests; MAF dbSNP and SIFT score using cut offs scores of <0.1 for each test and the variants in intersection portion of three tests were selected as final list.

Determination of cell growth rate in each cell fractions from WM cell lines

FACS-sorted cells (5×10^4 cells per well for MWCL-1 cells; 2.5×10^4 cells per well for BCWM.1 cells) were seeded in 96-well plates and were cultured independently in the absence of mitogenic or cytokine stimulation for 72 h. A lower number of BCMW.1 sorted cells were seeded compared with MWCL-1 sorted cells to prevent the cell death during the 72 h of nutrient deprivation, because the doubling time of BCWM.1 cells is approximately 3-fold shorter is shorter than that of MWCL-1 cells. Cells were enumerated at the start and the end of culture to determine proliferation and differentiation.

To determine the number of cells 72 h after culture without stimuli, 10 μL of 123count eBeads (ThermoFisher) was added to each sample of antibody-stained cells prior to flow cytometric analysis. The number of beads was counted at same time as flow cytometric analysis and cell counting for WM cell lines with a BD APF LSRII cytometer (BD Biosciences).

The number of cells in the 200 μL of sample was then determined as follows:

Absolute count (cells/μL)

= [(Cell count X eBeads volume)/(eBead count X Cell volume)] x (eBeads Concentration)

ELISA

The sorted PC and LPC populations from the two cell lines were plated in a 96-well plate at a density of 1×10^6 cells/mL in 200 μL and cultured in RPMI-1640 containing 10% FBS and 1 × antibiotic-antimycotic (ThermoFisher) without stimuli for 72 h. Cell-free supernatants were collected from each well and the IgM concentration was determined using the human IgM ELISA kit (Abcam, UK) according to the manufacturers' instructions. The optical densities were measured with an infinite M200PRO (TECAN, Switzerland) at a wavelength of 450 nm and at 570 nm as reference. The concentration of IgM was calculated from an IgM standard curve.

QUANTIFICATION AND STATISTICAL ANALYSIS

Statistical analysis

Statistical analyses were performed using PRISM 9.0. Statistical significance was defined as NS, not statistically significant and $p > 0.05$; *$p < 0.05$ and **$p < 0.01$. One-way ANOVA was used to analyse IgM secretion among samples. Pearson's correlation coefficient was used to measure the association between IgM secretion and number of PCs. Data are presented as mean ± S.D. The details of statistical tests are provided in the relevant results section and figure legends.